Supporting information

Facile synthesis of nanosized mordenite and Beta zeolites with improved catalytic performance: non-surfactant diquaternary ammonium compounds as organic structure-directing agents

Shaojie Li, Rim C. J. van de Poll, Nikolay Kosinov, and Emiel J. M. Hensen*

Laboratory of Inorganic Materials and Catalysis
Department of Chemical Engineering and Chemistry
Eindhoven University of Technology
P. O. Box 513, 5600 MB Eindhoven, The Netherlands

*Corresponding author
E-mail address: e.j.m.hensen@tue.nl

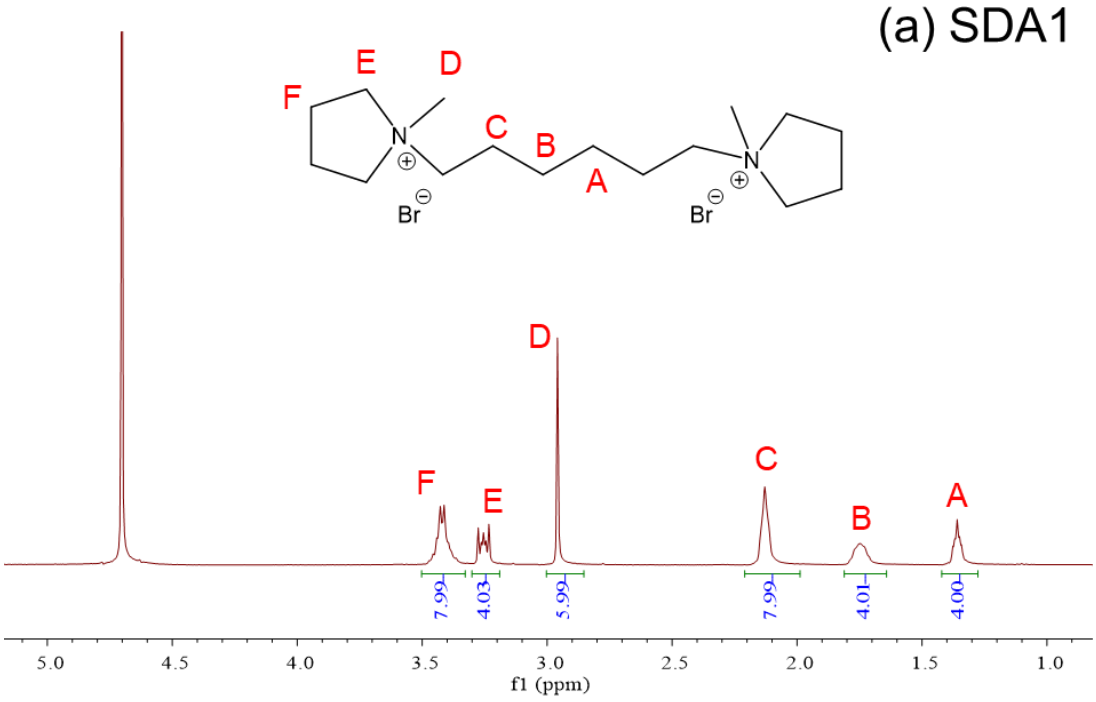
(a) SDA1
F
E
D
C
B
A
N
Br
D
F
E
C
B
A
7.99
4.03
5.99
7.99
4.01
4.00
5.0
4.5
4.0
3.5
3.0
2.5
2.0
1.5
1.0
f1 (ppm)

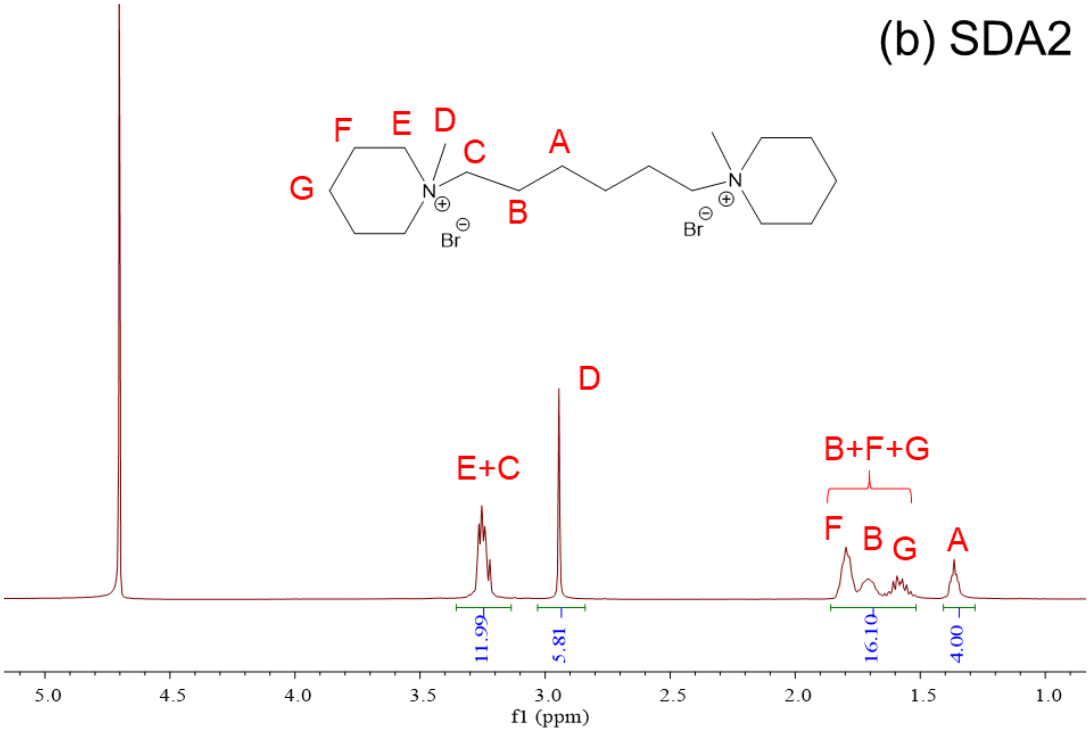
(b) SDA2
F
E
D
C
A
G
B
N
Br
D
E+C
B+F+G
F
B
G
A
11.99
5.81
16.10
4.00
5.0
4.5
4.0
3.5
3.0
2.5
2.0
1.5
1.0
f1 (ppm)

(c) SDA3

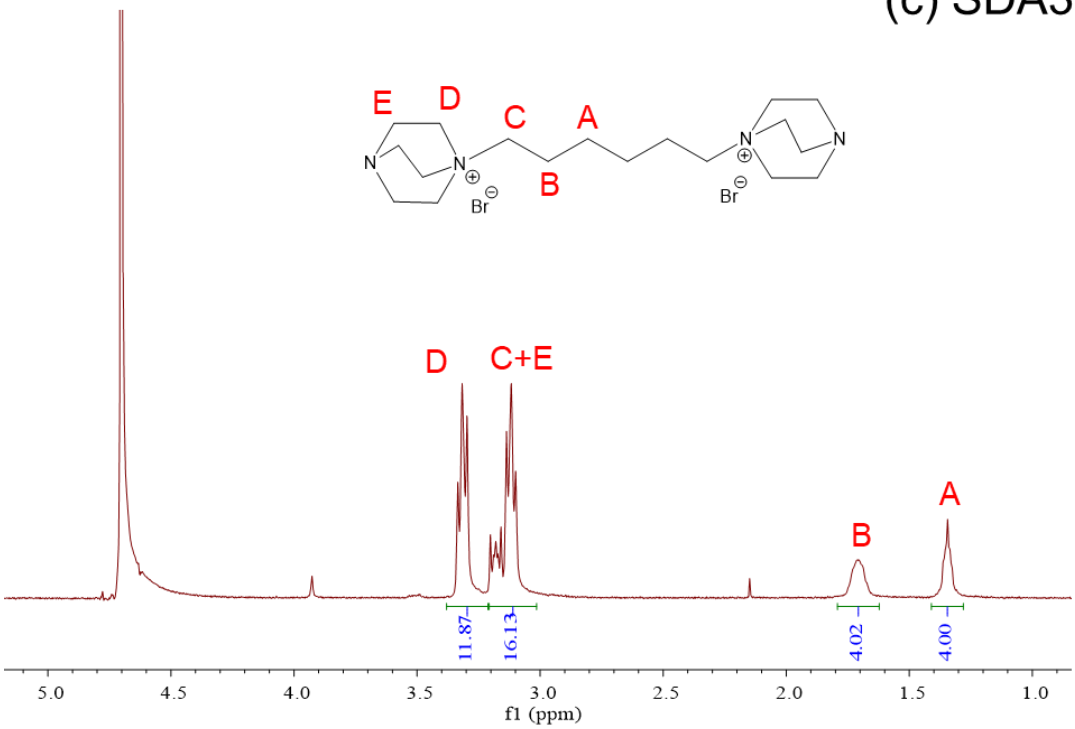
E
D
C
A
B
N
N
Br
N
N
Br
D
C+E
B
A
11.87
16.13
4.02
4.00
5.0
4.5
4.0
3.5
3.0
2.5
2.0
1.5
1.0
f1 (ppm)

(d) SDA4

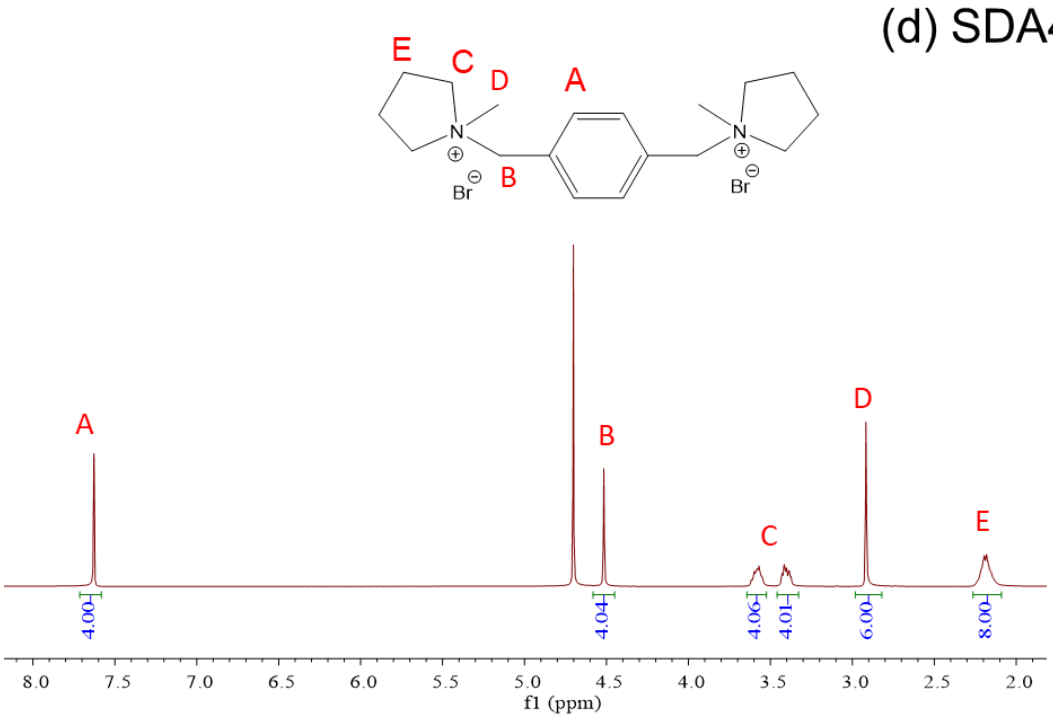
E
C
D
A
B
N
N
Br
Br
A
B
C
D
E
4.00
4.04
4.06
4.01
6.00
8.00
8.0
7.5
7.0
6.5
6.0
5.5
5.0
4.5
4.0
3.5
3.0
2.5
2.0
f1 (ppm)

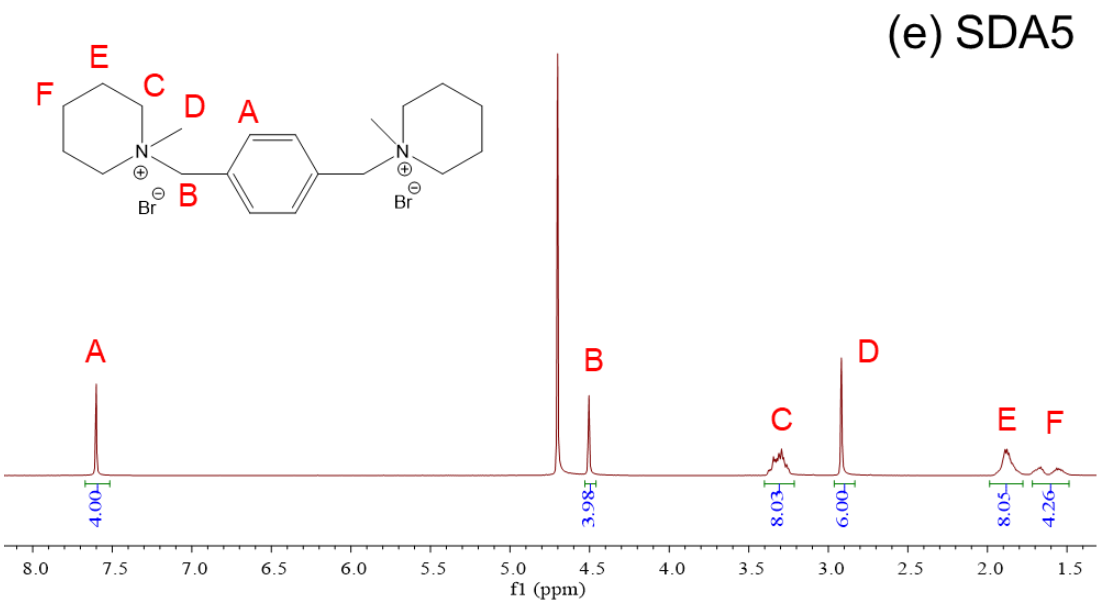

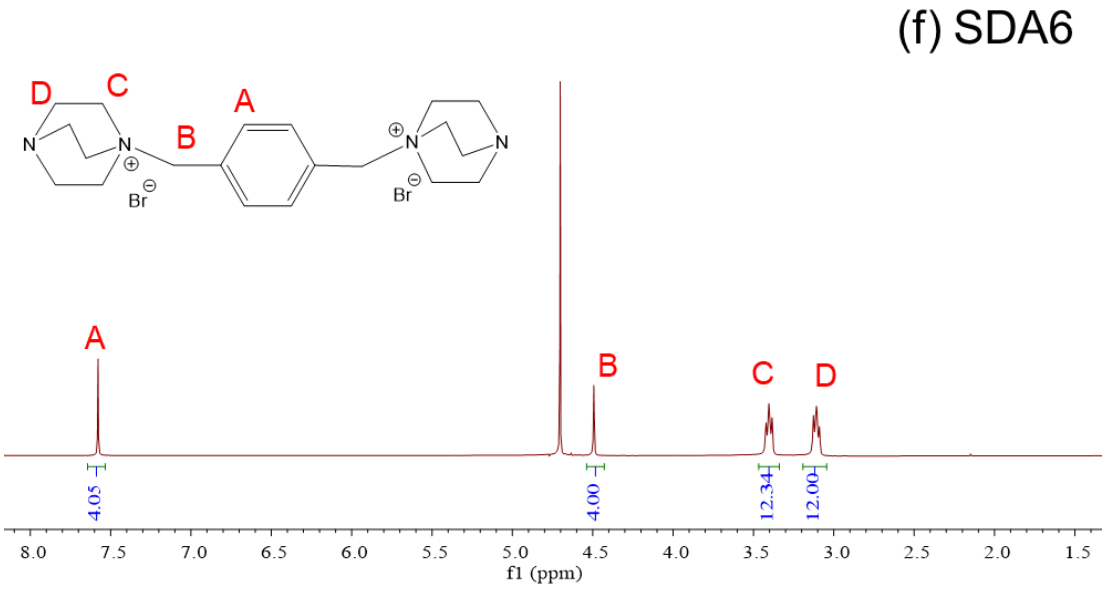

Fig. S1. Liquid-state ^{1}H NMR spectra of organic structure-directing agents (SDA) used in this work.

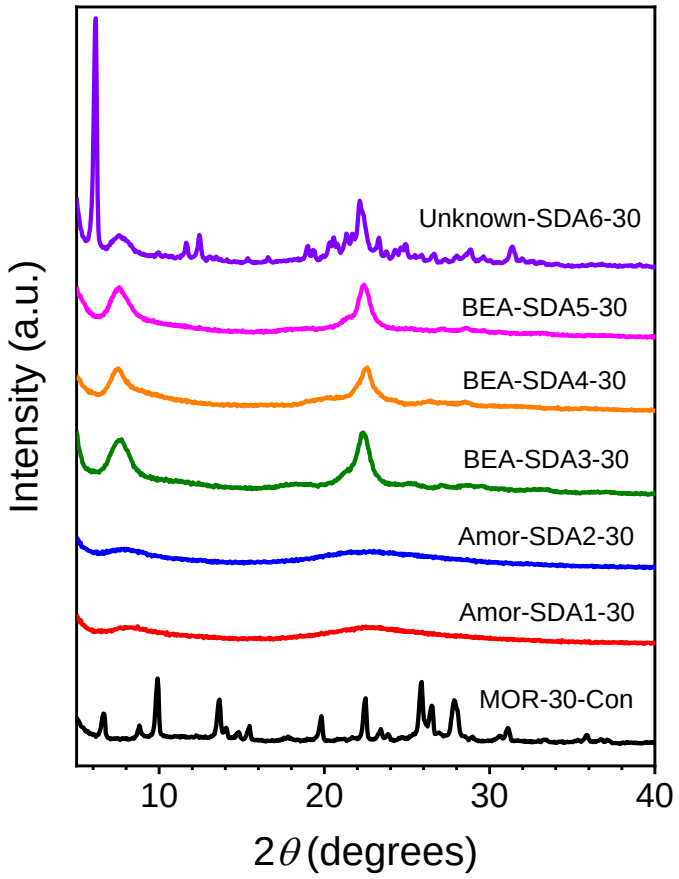

Fig. S2. XRD patterns of samples synthesized using the templates shown in Fig. 1 (recipe: Si/Al = 30).

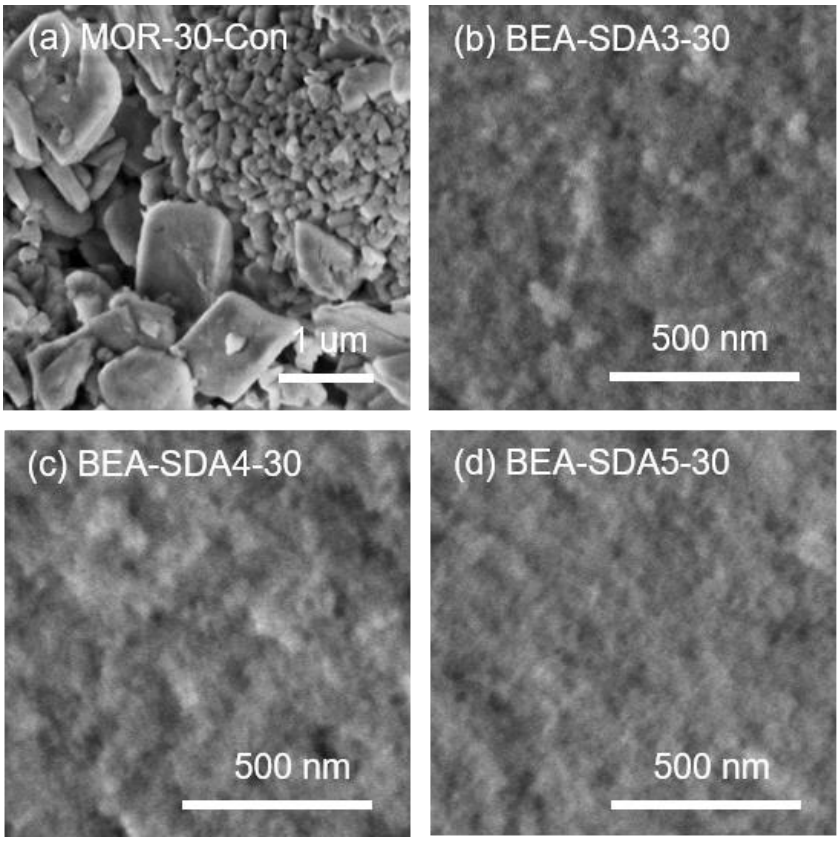

Fig. S3. SEM images of calcined zeolites (recipe: Si/Al=30).

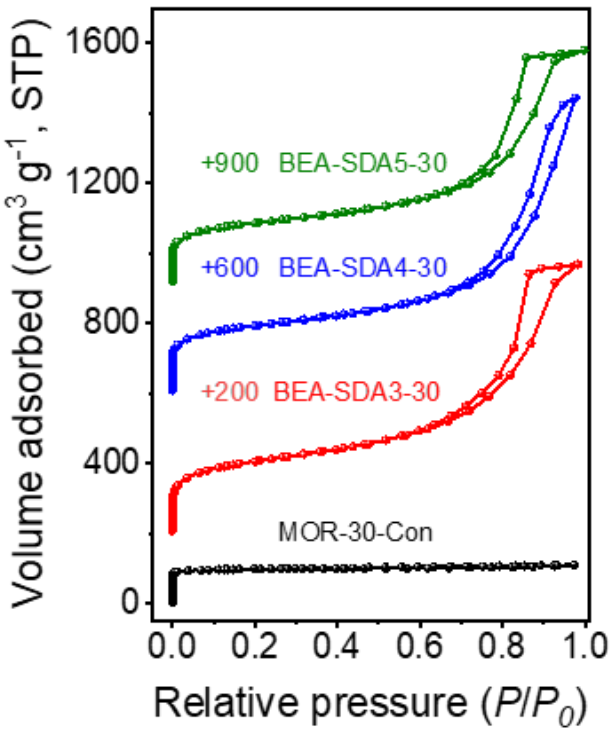

Fig. S4. Ar physisorption isotherms of calcined zeolites (recipe: Si/Al=30).

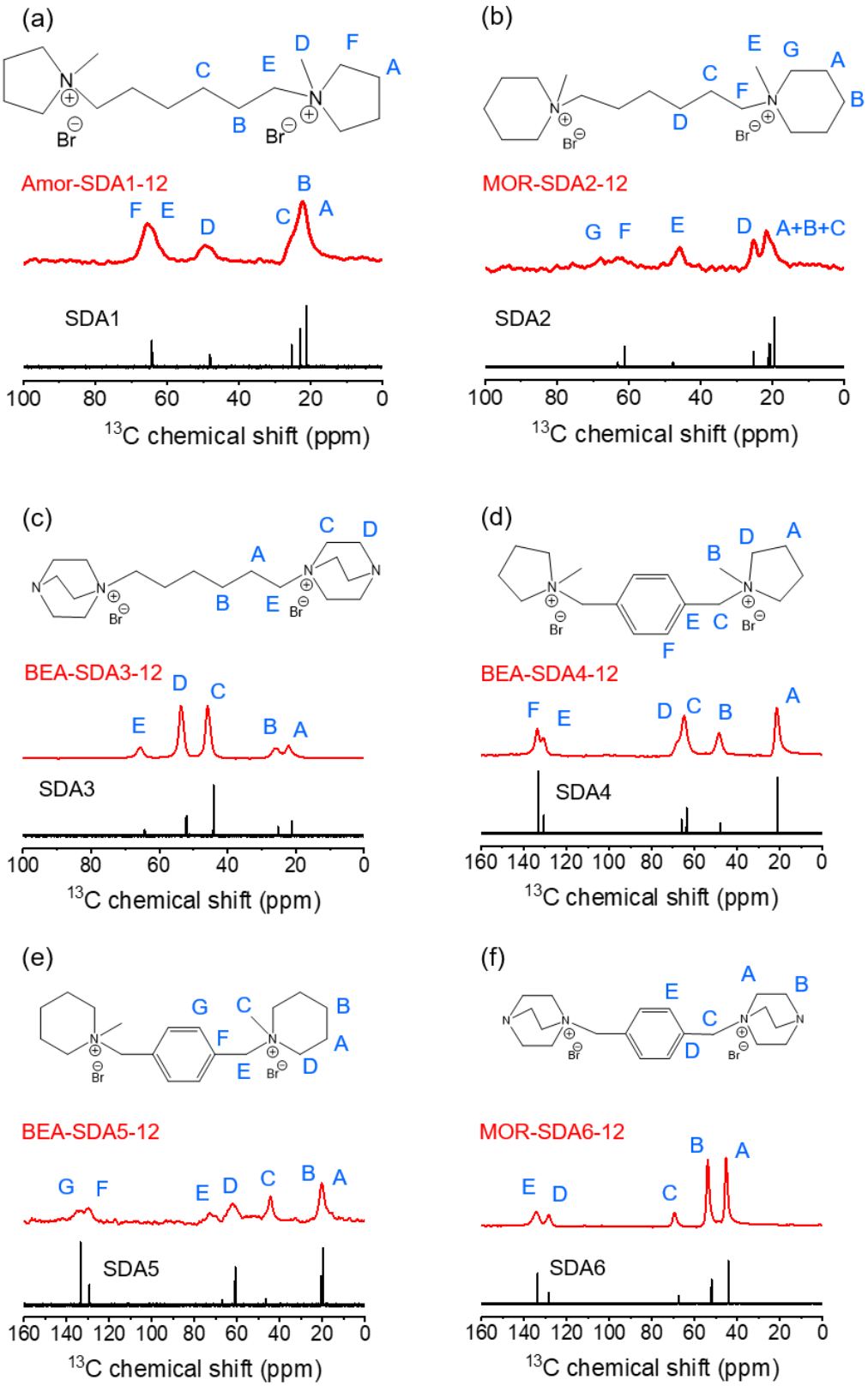

Fig. S5. Liquid-state ^{13}C NMR spectra (red line) of SDA in D_2O solution: (a) SDA1, (b) SDA2, (c) SDA3, (d) SDA4, (e) SDA5 and (f) SDA6; Solid-state ^{1}H-^{13}C CPMAS NMR spectra (black line) of as-prepared samples: (a) Amor-SDA1-12; (b) MOR-SDA2-12; (c) BEA-SDA3-12; (d) BEA-SDA4-12; (e) BEA-SDA5-12 and (f) MOR-SDA6-12.

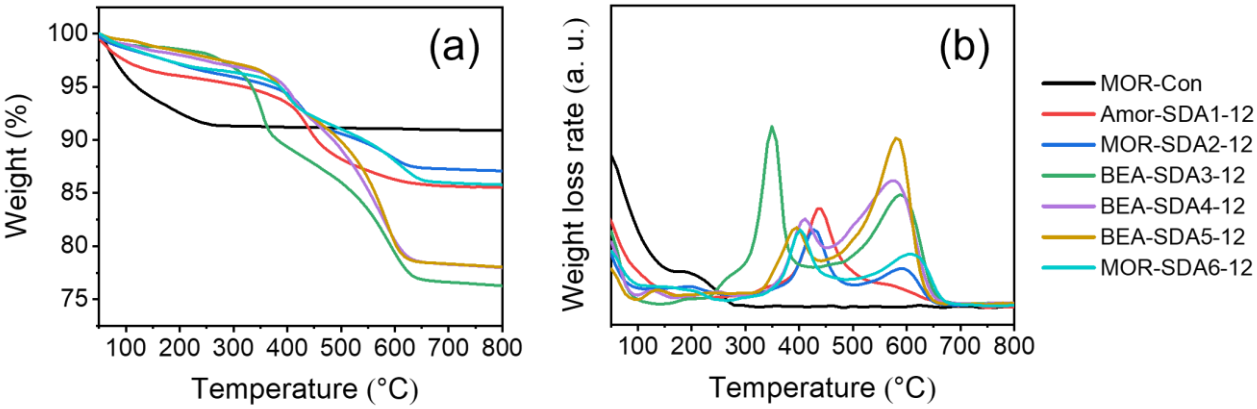

Fig. S6. (a) TG and (b) DTG of as-prepared samples.

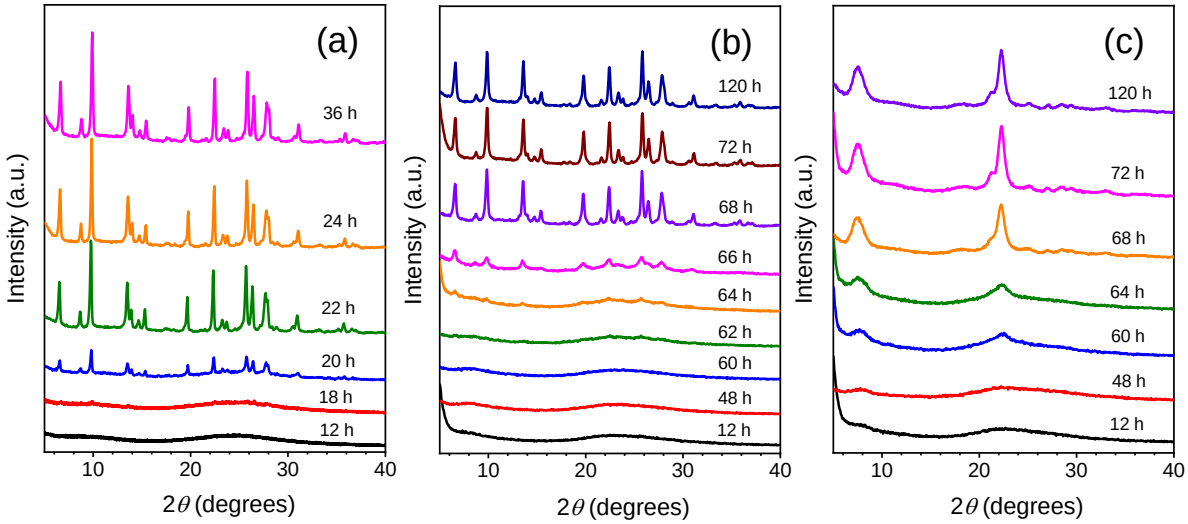

Fig. S7. XRD patterns of solid samples obtained at different crystallization times: (a) MOR-12-Con, (b) MOR-SDA2-12 and (c) BEA-SDA3-12.

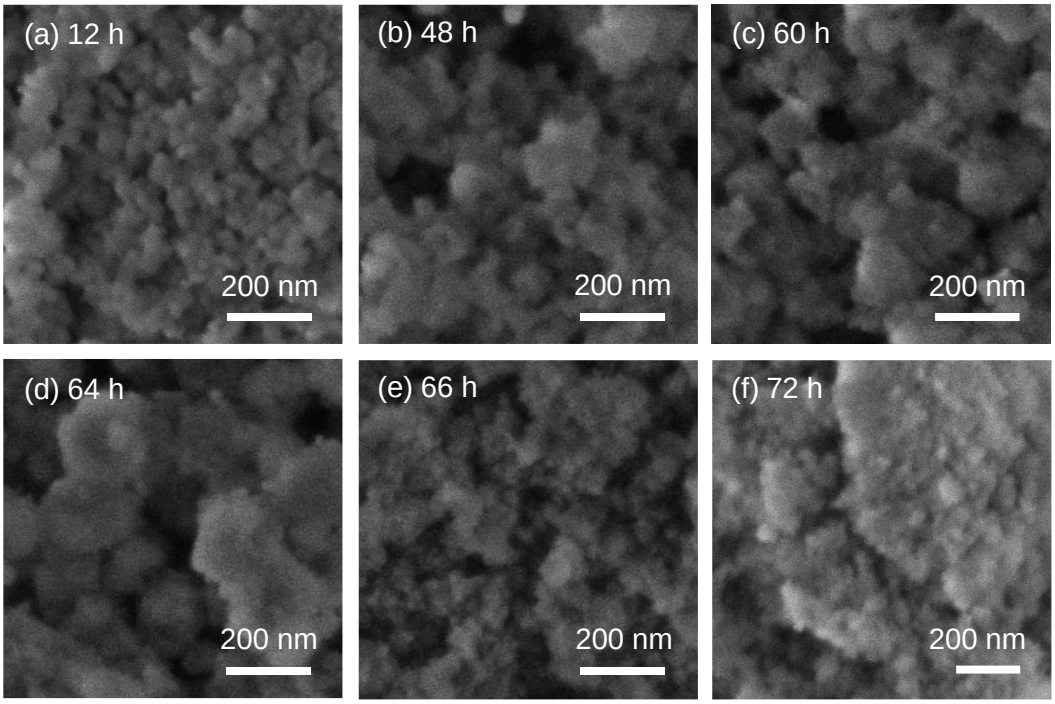

Fig. S8. SEM images of solid samples obtained at different crystallization times of BEA-SDA3-12.

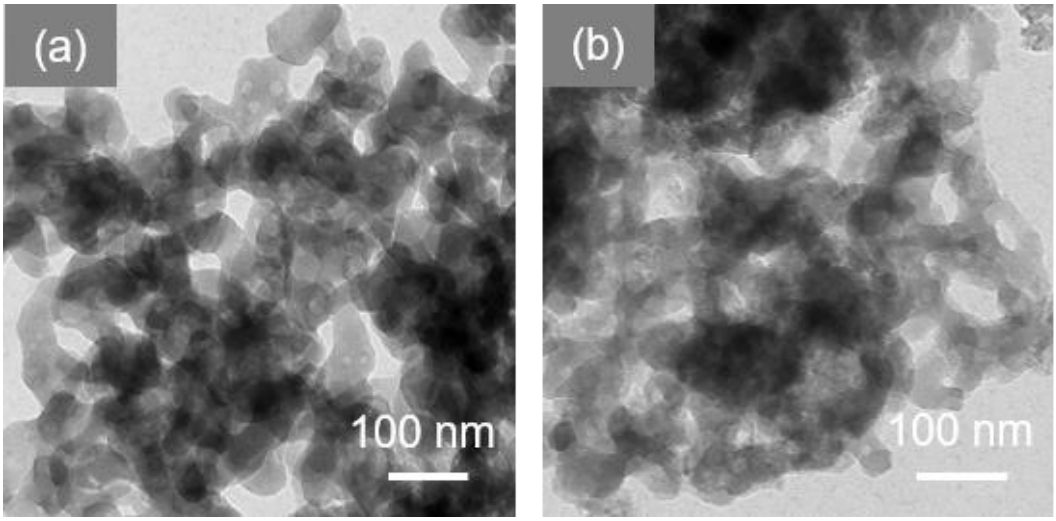

Fig. S9. TEM images of solid products: (a) MOR-SDA2-12-(48 h) and (b) BEA-SDA3-12-(48 h).

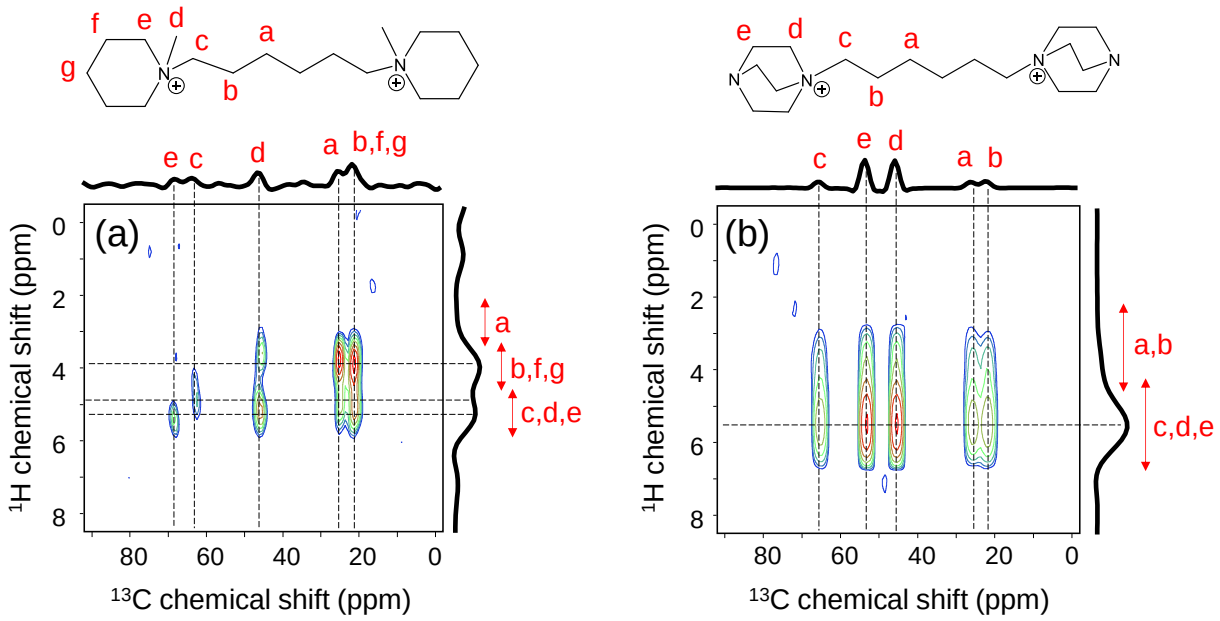

Fig. S10. ^{1}H-^{13}C HETCOR NMR spectra of as-prepared zeolites: (a) MOR-SDA2-12 and (b) BEA-SDA3-12 (assignment to different H atoms in SDA in top panels).

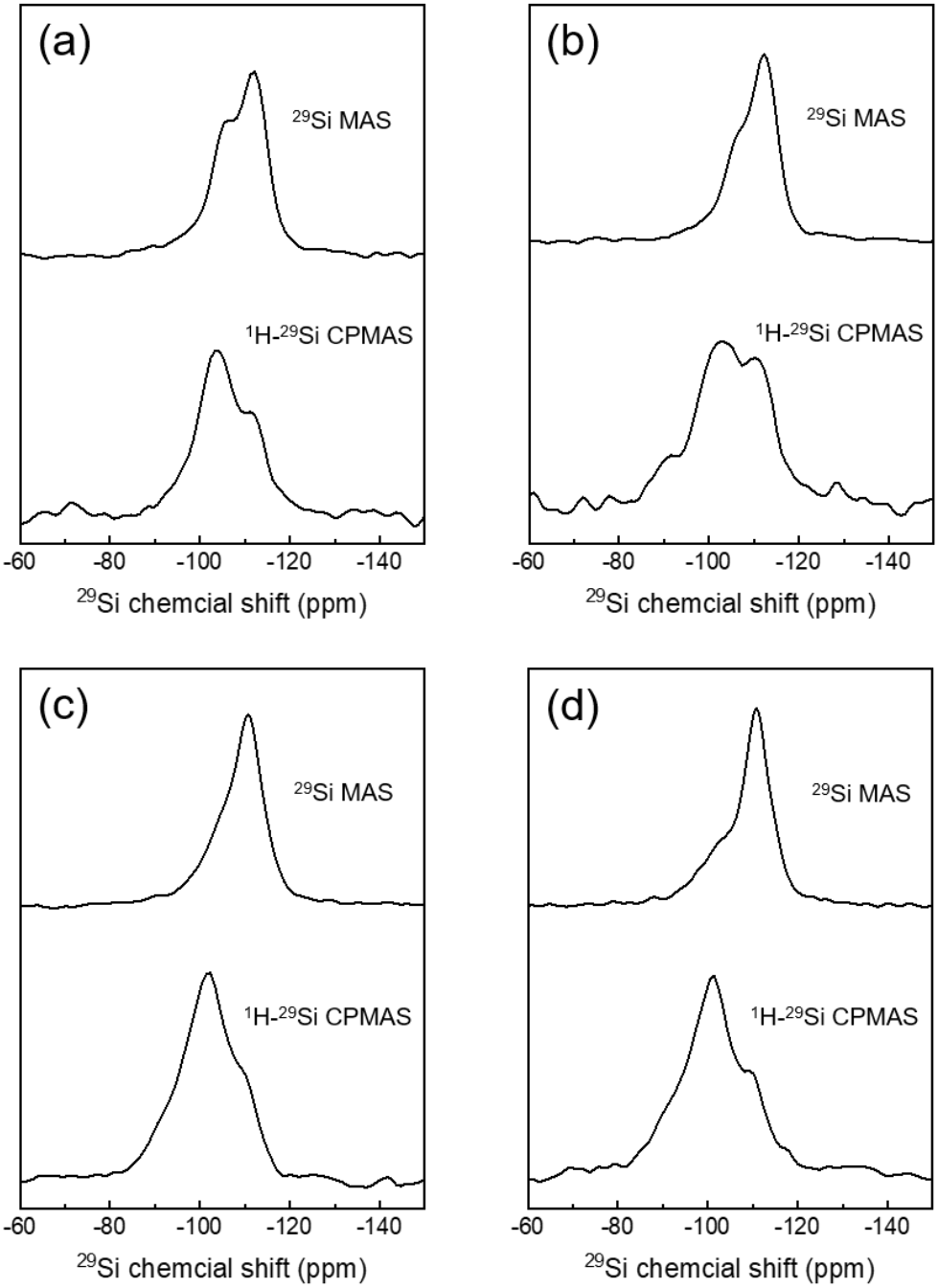

Fig. S11. ^{29}Si MAS NMR and ^{1}H-^{29}Si CPMAS spectra of the calcined zeolites: (a) MOR-12-Con, (b) MOR-SDA2-12, (c) BEA-12-Con and (d) BEA-SDA3-12.

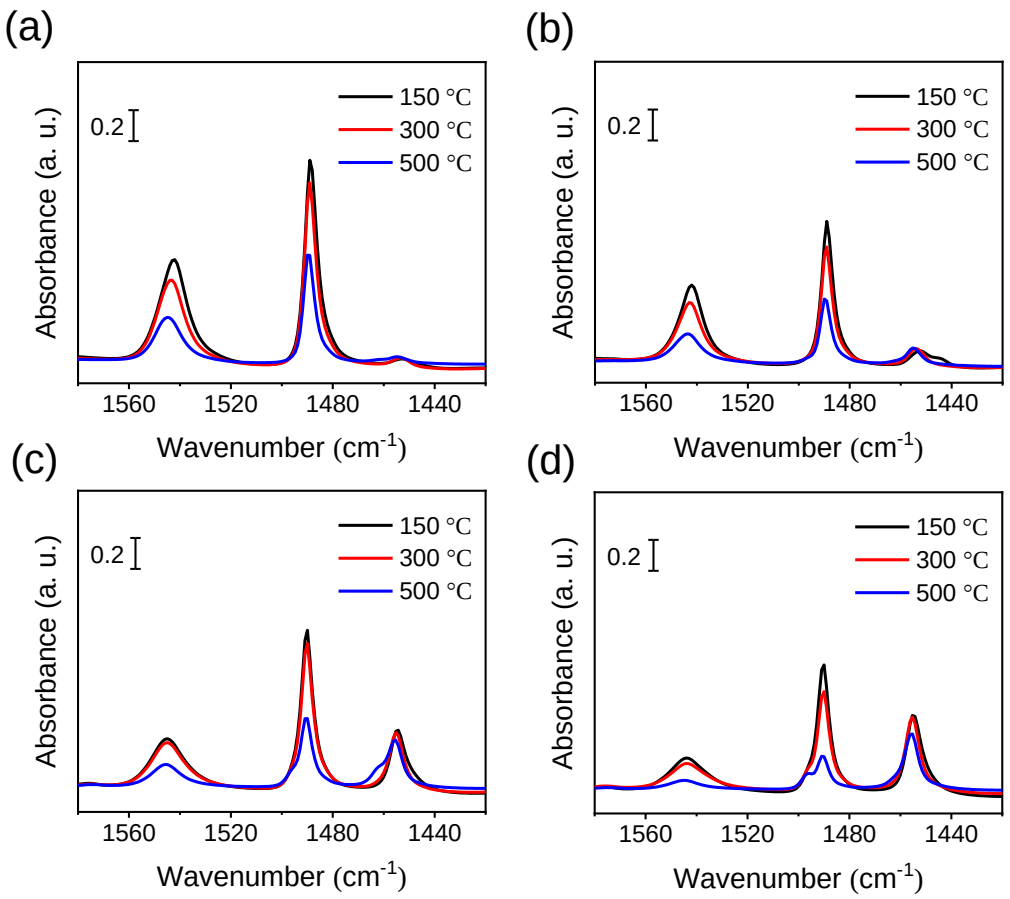

Fig. S12. IR spectra of pyridine adsorbed on zeolites: (a) MOR-12-Con, (b) MOR-SDA2-12, (c) BEA-12-Con and (d) BEA-SDA3-12.

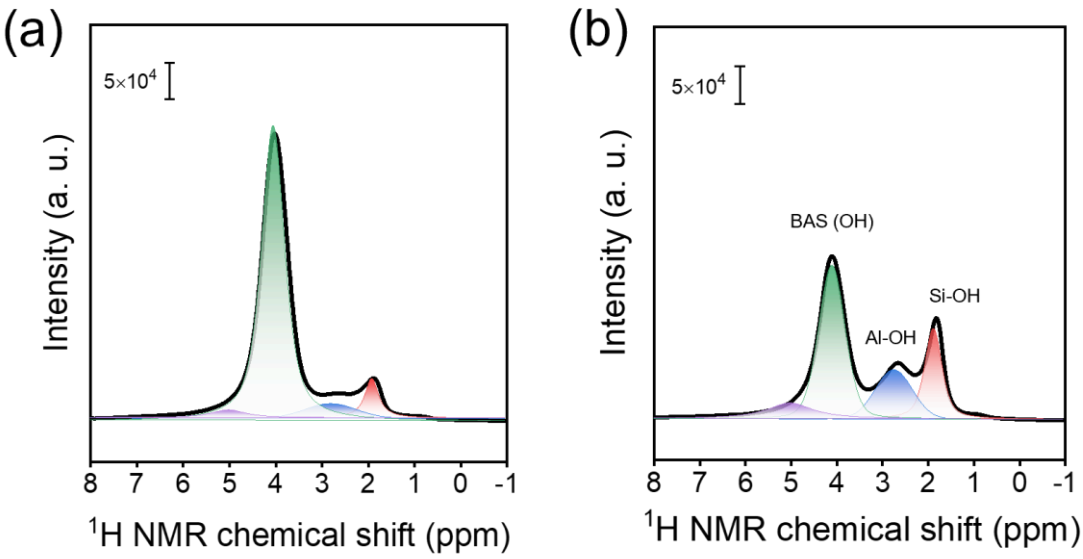

Fig. S13. ^{1}H NMR spectra of dehydrated samples: (a) MOR-12-Con and (b) MOR-SDA2-12.

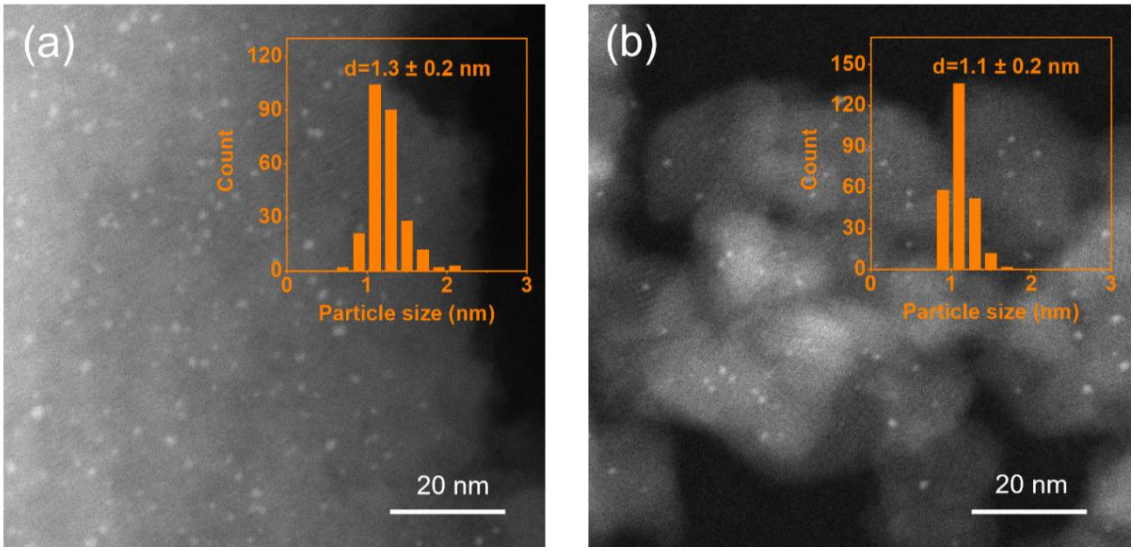

Fig. S14. ADF-STEM images of reduced samples: (a) Pt/BEA-12-Con and (b) Pt/BEA-SDA3-12.

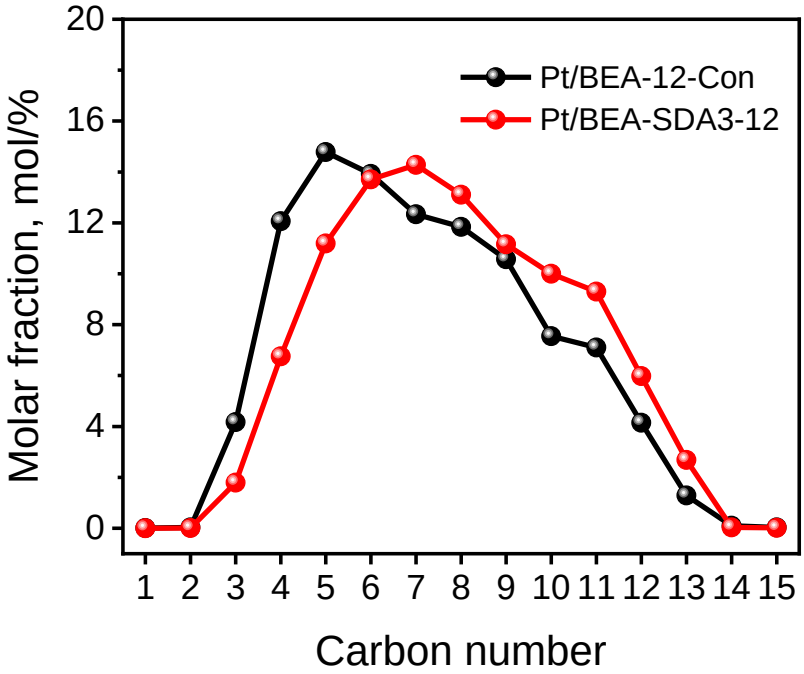

Fig. S15. The distribution of cracked products at ca. 50% n-C_{16} conversion.

Table S1. Prices of chemicals used for organic template synthesis.

Chemical	Supplier	Price
1,6-dibromohexane	TCI, > 97.0%	52.00 €/500 g
α,α′-dibromo-*p*-xylene	TCI, > 98.0%	64.00 €/25 g
N-methypyrrolidine	TCI, > 98.0%	80.00 €/500 ml
N-methylpiperidine	TCI, > 99.0%	90.00 €/500 ml
1,4-diazabicyclo[2.2.2]octane	TCI, > 98.0%	91.00 €/500 g

Table S2. Solid yields and Si/Al ratios of zeolite samples obtained at a Si/Al gel ratio of 12.

Zeolite	Si/Al	Yield (%)
MOR-12-Con	8.4	69.9
MOR-SDA2-12	9.2	76.6
MOR-SDA6-12	9.8	81.1
BEA-SDA3-12	11.7	75.3
BEA-SDA4-12	11.9	60.3
BEA-SDA5-12	12.0	64.1
BEA-12-Con	11.3	59.7

Table S3. Solid yields and Si/Al ratios of zeolite samples obtained at a Si/Al gel ratio of 30.

Zeolite	Si/Al	Yield (%)
MOR-30-Con	13.4	43.4
BEA-SDA3-12	14.3	35.1
BEA-SDA4-12	15.8	51.4
BEA-SDA5-12	14.9	41.7

Table S4. Textural properties of calcined zeolites determined by Ar physisorption.

Zeolite	S_{BET} ($m^2 g^{-1}$)	V_{tot} ($cm^3 g^{-1}$)	V_{meso} ($cm^3 g^{-1}$) (*BJH*)	V_{micro} ($cm^3 g^{-1}$) (*t-plot*)	S_{ext} ($m^2 g^{-1}$) (*t-plot*)
MOR-30-Con	303	0.14	0.02	0.12	37
BEA-SDA3-30	648	0.98	0.79	0.10	370
BEA-SDA4-30	604	1.08	0.90	0.11	313
BEA-SDA5-30	549	0.85	0.69	0.10	295

Table S5. Changes in the solid yield and chemical compositions along with the synthesis time for MOR-12-Con.

Synthesis time (h)	Solid yield (wt %)	Si/Al
12	77.3	9.0
18	77.1	9.1
20	75.0	8.8
24	69.9	8.4

Table S6. Changes in the solid yield and chemical compositions along with the synthesis time for MOR-SDA2-12.

Synthesis time (h)	Solid yield (wt %)	Si/Al	Organic content (wt %)
12	75.1	9.1	8.7
60	74.7	9.2	9.2
66	76.0	9.1	9.6
72	76.6	9.2	9.1

Table S7. Changes in the solid yield and chemical compositions along with the synthesis time for BEA-SDA3-12.

Synthesis time (h)	Solid yield (wt %)	Si/Al	Organic content (wt %)
12	76.2	9.2	11.8
48	78.2	9.4	12.3
60	79.5	10.1	15.4
72	75.3	11.7	21.5

Table S8. Al and Si distributions of the proton form zeolites.

Zeolite	^{27}Al NMR[a]		^{29}Si NMR			Si/Al$_F$[b]
	Al^{IV}	Al^{VI}	Q^4(2Al)/ Q^3(0Al)	Q^4(1Al)	Q^4(0Al)	
MOR-12-Con	80	20	13	33	54	6.8
MOR-SDA2-12	83	17	10	27	63	8.5
BEA-12-Con	74	26	5	28	67	10.5
BEA-SDA3-12	70	30	7	25	68	10.3

[a]Al^{IV} determined by integration of NMR signal between 20 and 100 ppm; Al^{VI} determined by integration of NMR signal between 20 and -50 ppm.

[b]Framework Si/Al=2 Σ ISi(nAl)/ Σ0.25·n·ISi(nAl) with assuming that Q^3(0Al) does not contribute to the intensity of Q^4(2Al)/ Q^3(0Al), n = 0-4.

Table S9. BAS distribution derived from deconvoluted IR spectra of MOR zeolites.

Zeolite	BAS in 8MR (%)	BAS in 8/12MR (%)	BAS in 12MR (%)
MOR-12-Con	49	30	21
MOR-SDA2-12	64	25	11

Table S10. Catalytic performance of the acylation of anisole with anhydride over BEA zeolites after 6 h reaction.

Zeolite	Acetic anhydride conversion (%)	*p*-MAP yield (selectivity) (%)
BEA-12-Con	48	39 (81)
BEA-SDA3-12	67	57 (85)

p-MAP: *p*-methoxyacetophenone

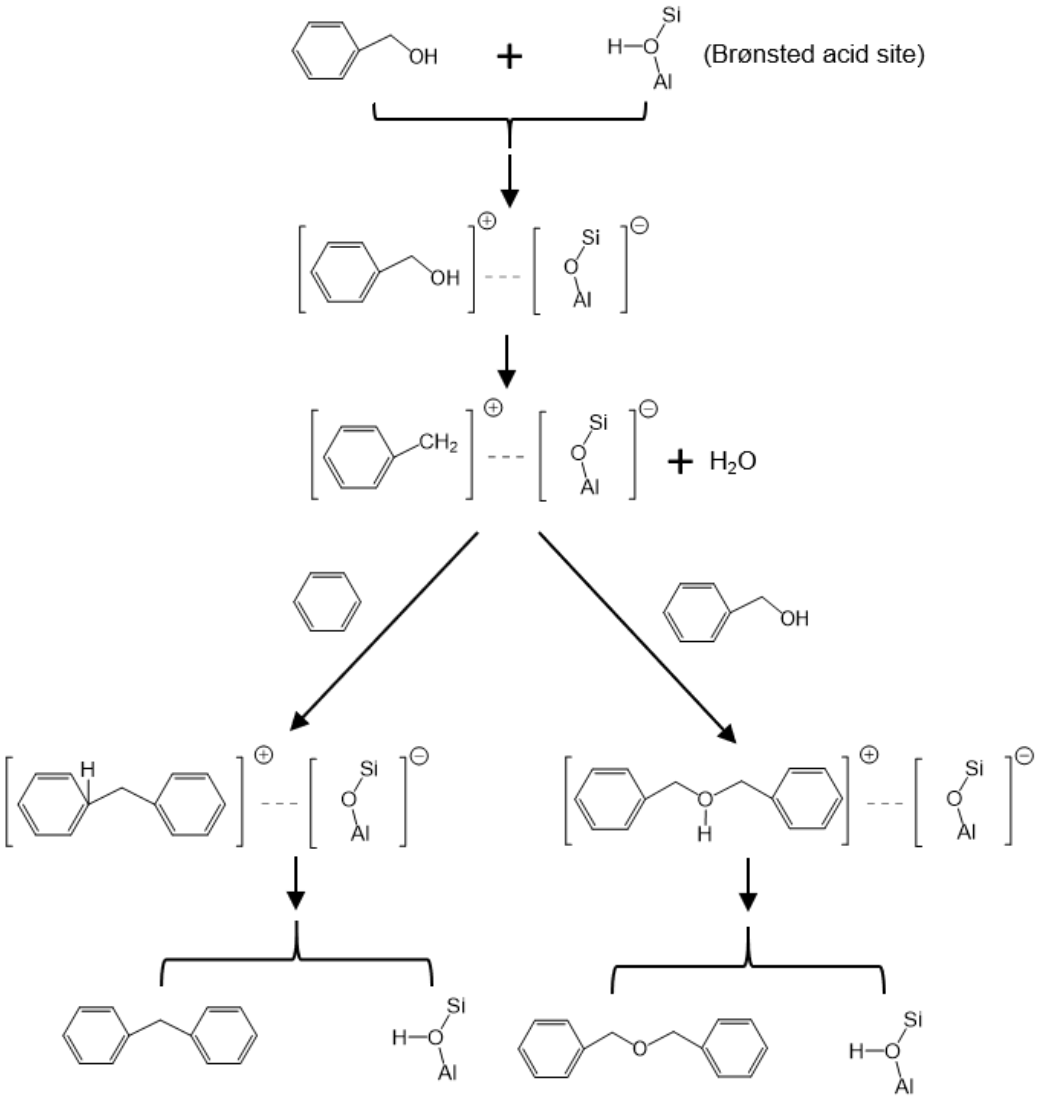

Scheme S1. Reaction pathways for benzylation of benzene with benzyl alcohol.

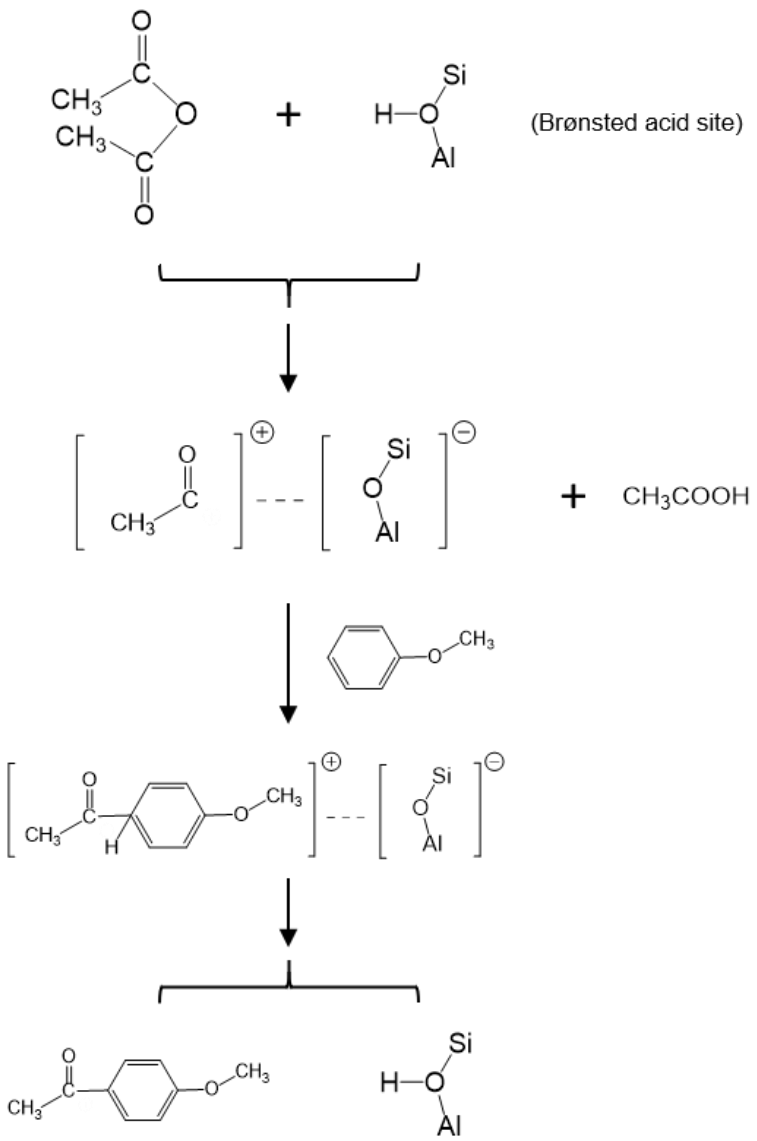

Scheme S2. Reaction pathway for acylation of anisole with acetic anhydride (*p*-methoxyacetophenone as the product).